JOURNAL OF MATERIALS SCIENCE 22 (1987) 2481–2492

The abrasive wear behaviour of continuous fibre polymer composites

M. CIRINO, R. B. PIPES
Center for Composite Materials, University of Delaware, Newark, Delaware, USA
K. FRIEDRICH
Polymer and Composites Group, Technical University Hamburg-Harburg, Hamburg, West Germany

The dry abrasive-dominant wear behaviour of several composite materials consisting of unidirectional continuous fibres and polymer matrices was investigated. Seven materials were examined: neat epoxy (3501-6), carbon fibre epoxy (AS4/3501-6), glass fibre/epoxy (E-glass/3501-6), aramid fibre/epoxy (K49/3501-6), neat polyetheretherketone (PEEK), carbon fibre/PEEK (APC2) and aramid fibre/PEEK (K49/PEEK). The wear behaviour of the materials was characterized by experimentally determining the friction coefficients and wear rates with a pin-on-flat test apparatus. First, the effects of the operation variables apparent normal pressure, sliding velocity and apparent contact area were observed. The dimensionless wear rate increased linearly as the apparent normal pressure increased and decreased as the apparent contact area increased. Second, through microscopic observations of the worn surfaces and subsurface regions, basic wear mechanisms were identified as a function of fibre orientation. Observations of fibre–abrasive particle interactions allowed for the differentiation of the dominating wear mechanisms. Finally, a network of data was compiled on the wear behaviour in terms of the three material parameters: fibre orientation, fibre material and matrix material. This enabled the systematic selection of an ideal low wear composite material which would consist of a PEEK matrix reinforced with aramid fibres oriented normal to the contacting surface and carbon fibres oriented parallel to the contacting surface.

1. Introduction

Advanced composite materials have gained increased attention in tribological applications. Along with their excellent structural performance, fibre-reinforced polymers excel in highly abrasive-type systems such as conveyor aides and chute liners in agricultural, mining and earth-moving equipment. Yet, the need for a fundamentally comprehensive understanding of the abrasive wear behaviour of fibre-reinforced polymers still exists. The majority of the papers in the past have concentrated on the sliding-type systems [1–5]. Sung and Suh [6] demonstrated that anisotropic wear behaviour was present in continuous fibre-reinforced polymers. Tsukizoe and Ohmae [7] investigated the wear behaviour of composites incorporating several different fibre materials. The counterface on which the composite material slides has been shown to effect the resulting wear behaviour by Tanaka [8]. On the other hand, abrasive-type wear investigations are limited. A few studies have been done for unreinforced polymers [9–12] and short, fibre-reinforced polymers [13, 14]. Friedrich [15] has classified the dominant micro-wear mechanisms which occur during abrasive wear of different polymers and polymer composites. A common conclusion among the majority of friction and wear studies is that the wear resistance of a material cannot be considered as an intrinsic property; rather, it strongly depends on the system in which the materials function (Fig. 1). In this paper, a systematic investigation of the wear performance of selected polymer composites under dry abrasive conditions is considered. The main interest is the effect of various types of fibre reinforcements on the wear resistance of polymer matrices of different mechanical properties.

2. Experimental details

2.1. Materials

Seven material systems were employed in the friction and wear tests whose constituents included two matrix materials and three fibre materials. The composite systems consisted of carbon/epoxy (CF–EP), glass/epoxy (GF–EP), aramid/epoxy (AF–EP), aramid polyetheretherketone (i.e. aramid/PEEK (AF–PK)) and carbon/polyetheretherketone (i.e. carbon/PEEK (CF–PK)) which are described in more detail in Table I. The epoxy systems were fabricated in an autoclave using the cure cycle recommended by the manufacturer. The CF–PK system was fabricated using a compression press following the procedure suggested by the manufacturer. The AF–PK system was the only composite which was not self-manufactured, but was directly received as a preliminary laboratory product from ICI, Wilton, U.K. [16]. All composite systems consisted of unidirectional

0022–2461/87 $03.00 + .12

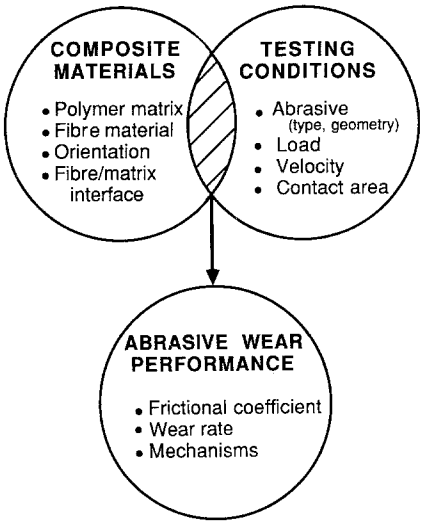

Figure 1 The dependence of wear on the system.

continuous fibres. Accordingly, three fibre orientations were obtained with respect to the sliding surface for each composite system as depicted in Fig. 2. The normal orientation (N) is defined as when the fibres are perpendicular to the sliding surface. The parallel orientation (P) is defined as when the fibres are parallel to the sliding direction. The antiparallel orientation (AP) is defined as when the fibres are perpendicular to the sliding direction and parallel to the sliding surface plane.

For each material system a nominally 3.2 mm thick plate was appropriately fabricated from which cubic systems were cut. This produced an average apparent contact area (A) of approximately 10 mm^2. For the special cases where the apparent contact area was greater than 10 mm^2 the specimens were no longer cubic. They were cut such that the contacting surface was of a square geometry and the depth was kept constant at about 3.2 mm.

2.2. Testing procedures

A pin-on-flat type apparatus was designed and fabricated by the authors. A simplified schematic illustration is shown in Fig. 3. A more detailed description of the apparatus is given in [17]. The counterface material was adhered to the mill table. One hundred eighty grit and six hundred grit silica carbide (SiC) abrasive paper manufactured by the Buehler company

TABLE I Materials employed in the friction and wear tests

Abbreviation	Material	Fibre volume fraction (%)	Density ($g\,cm^{-3}$)
Thermoset			
EP	Epoxy resin	–	1.28
CF–EP	AS4 carbon fibre/epoxy	62	1.59
GF–EP	E-glass fibre/epoxy	58	2.01
AF–EP	K49 aramid fibre/epoxy	60	1.34
Thermoplastic			
PK	polyetheretherketone (PEEK)	–	1.56
CF–PK	AS4 carbon fibre/PEEK	55	1.27
AF–PK	K49 aramid fibre/PEEK	60	1.38

was used. According to the manufacturer, the average particle diameters (D) were 70 and 15 μm, respectively. Generally, the specimens were slid against the SiC paper at a constant velocity (V) of 300 mm min^{-1} and at an apparent normal pressure (p) of 2.2 MPa for a sliding distance (L) of 500 mm. Four runs in the same direction were made for each specimen. Each run was on a fresh track of SiC paper (single-pass conditions). The mass loss of the specimen was observed after each run on a Mettler analytical balance (0.1 mg) under the same environmental conditions as the test was conducted. All tests were performed in controlled laboratory air which was at about 22° C and 35% r.h.

A load cell continuously monitored the frictional force between the specimen contact surface and the SiC abrasive paper. Applying the Amonton–Coulomb law of dry friction, a coefficient of friction (μ) was calculated as,

$$\mu = F_f/F_n \quad (1)$$

where F_f is the measured frictional force and F_n is the applied normal load. The magnitude of the frictional force was averaged over the entire sliding distance of the test. Wear behaviour was characterized by defining a dimensionless wear rate (W) which relates volume loss (ΔV) to sliding distance (L) and apparent contact area (A) in the following manner

$$W = \Delta V/LA \quad (2)$$

The volume loss can be found by using the mass loss (Δm) and density (ϱ) measurements in the following

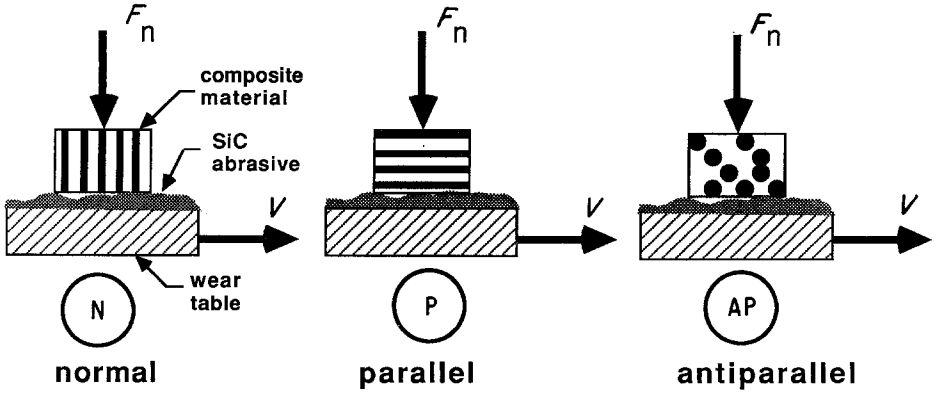

Figure 2 Three basic fibre orientations for continuous fibre-reinforced composites.

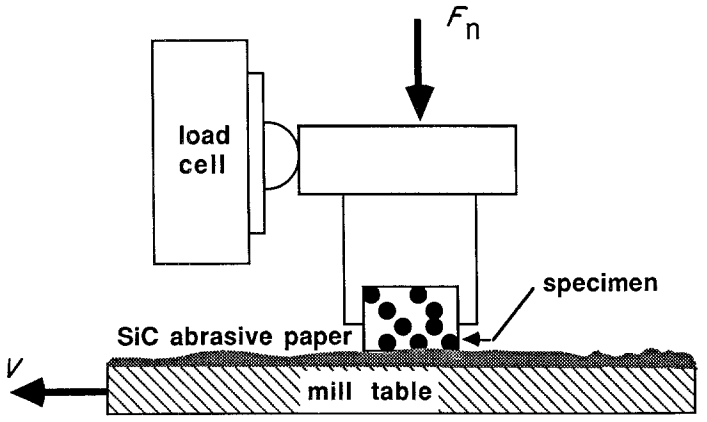

Figure 3 Simplified illustration of the pin-on-flat test apparatus.

form

$$\Delta V = \Delta m/\varrho \quad (3)$$

Inserting Equation 3 into Equation 2 yields a dimensionless wear rate which is defined by experimentally measured test parameters

$$W = \Delta m/\varrho LA \quad (4)$$

Dividing Equation 4 by the apparent normal pressure (p) yields the specific wear rate (W_s) as

$$W_s = W/p \quad (5)$$

which is given the dimensions of $mm^3 N^{-1} m^{-1}$. This describes the physical nature of the specific wear rate as a volume loss of material by a certain amount of energy input. Often, the wear resistance of a material is referred to which is simply the inverse of the wear rate (W^{-1} or W_s^{-1}).

2.3. Microscopy

Microscopic observations of the tested specimens were made by a scanning electron microscope (SEM). Special specimens were fabricated for the microscopy of the wear profiles of the composite materials allowing observations of the subsurface regions. A standard test specimen was cut in half, and the mating inner surfaces were polished to 1 μm. The specimen was placed in the specimen holder such that the mating inner surfaces were parallel to the clamping edges of the specimen holder. Also, the sliding direction was parallel to the mating inner surfaces. All surfaces which were microscopically observed under the scanning electon microscope were coated with a thin layer of gold following standard procedures for polymeric materials.

3. Test results

3.1. Effects of operating variables

The effects of varying the apparent normal pressure, the sliding velocity and the apparent contact area on the friction and wear performance were investigated. These tests were performed on the CF–EP system in the P orientation sliding against D = 70 μm SiC waterproof type abrasive paper. Figs 4 to 6 show no significant variations in the frictional coefficient for the ranges of operation variables considered. The dimensionless wear rate, on the other hand, increased in a linear fashion as the apparent normal pressure was increased from 1 to 4.4 MPa as shown in Fig. 7. A sliding velocity range of 100 to 350 mm min^{-1} did not have a significant effect on the dimensionless wear rate (Fig. 8). Fig. 9 illustrates that as the apparent contact area was increased from approximately 10 to 40 mm^2, the dimensionless wear rate decreased slightly. However, this behaviour may be due to the reduction in sharpness of the abrasive particles resulting from the enhanced wear of the particles as the distance it travels across the composite surface increases.

The type of SiC abrasive paper used as the counterface material was shown to effect the wear rates of

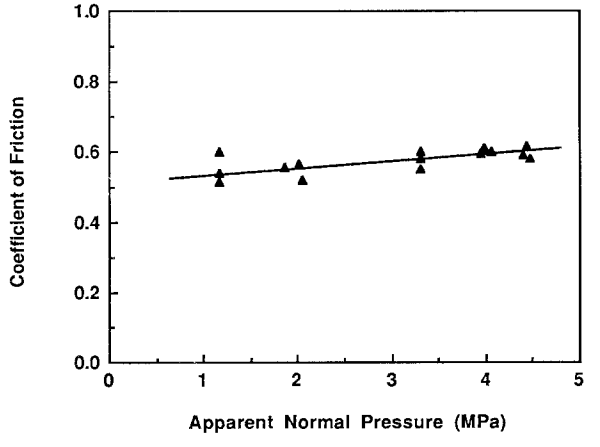

Figure 4 Coefficient of friction plotted against apparent normal pressure. CF–EP parallel orientation, V = 300 mm min^{-1}, A = 3 mm × 3 mm, D = 70 μm SiC.

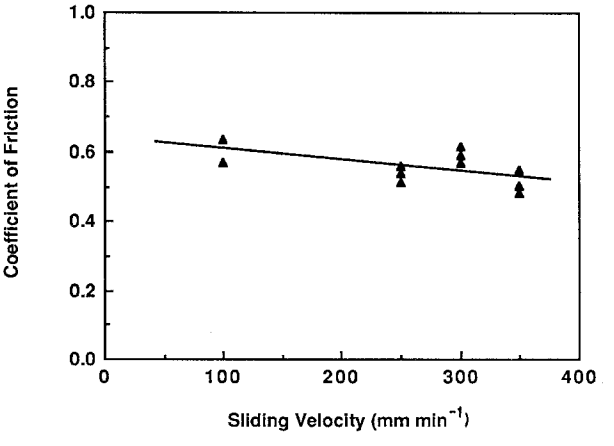

Figure 5 Coefficient of friction plotted against sliding velocity. CF–EP parallel orientation, p = 2.2 MPa, A = 3 mm × 3 mm, D = 70 μm SiC.

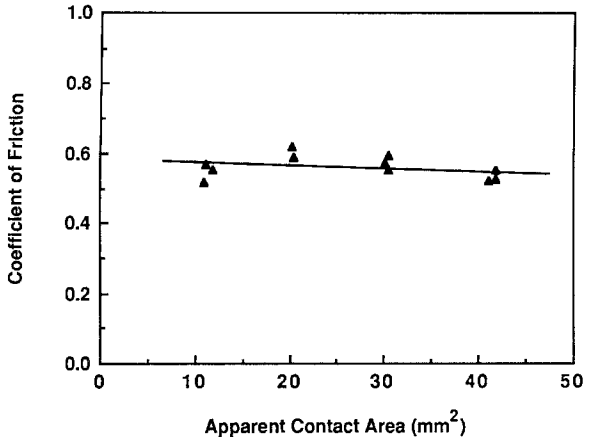

Figure 6 Coefficient of friction plotted against apparent contact area. CF–EP parallel orientation, p = 2.2 MPa, V = 300 mm min^{-1}, D = 70 μm SiC.

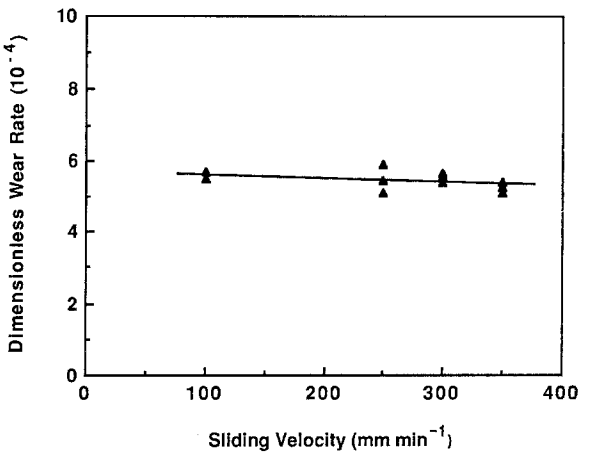

Figure 8 Dimensionless wear rate plotted against sliding velocity. CF–EP parallel orientation, p = 2.2 MPa, A = 3 mm × 3 mm, D = 70 μm SiC.

the AF–EP and CF–EP systems. Two types of SiC abrasive paper are commonly available which can be categorized as a "waterproof" and a "non-waterproof" type paper. The main difference between the two types of paper is that the waterproof type paper is provided with a protective coating which tends to fill the gaps in between adjacent particles leaving the particle tips exposed. This is clearly shown by the scanning electron micrographs of the D = 70 μm SiC waterproof and non-waterproof abrasive papers in Fig. 10. This paper effect was investigated to show that there does exist an influence on the wear rate, although, the exact dependence of the wear rate on this effect was not sought after. Table II illustrates this paper effect.

3.2. Wear behaviour of different composites

Anisotropic wear behaviour was especially evident among the composite systems sliding under the more abrasive condition (i.e. D = 70 μm) – see Figs 11 and 12. Fibre addition to the neat epoxy (EP) decreased the relative wear rate with the exception of the CF–EP and GF–EP systems in the AP orientation. Likewise, the frictional coefficient experienced a relative decrease upon fibre addition to the EP material. The wear rate of the neat PEEK (PK) was about half that of the EP. Unlike the epoxy systems, carbon fibre addition to the PEEK resulted in a relative increase in the wear rate and the coefficient of friction. Even though the two matrices show opposing trends in the relative wear rate due to carbon fibre addition, both the CF–EP and CF–PK systems were observed to exhibit the same magnitudes of wear rates. In general, the N orientation generated the lowest wear rates, and the AP orientation generated the highest wear rates among each fibre/matrix system. The optimum wear resistances were shown by the AF–EP and AF–PK systems when the fibres were in the N orientation.

The composite systems exhibited a lesser degree of anisotropy when sliding against the less abrasive paper (D = 15 μm) – see Figs 11 and 12. The measured wear rates were lower than those measured for the D = 70 μm case. Fibre addition to the EP material decreased the relative wear rates and the coefficients of friction. The wear rate of PK was lower than that of EP by a factor of about two. Also, carbon fibre addition proved to be favourable to the wear resistance of the PK material unlike the D = 70 μm case. Again, both carbon fibre-reinforced systems exhibited the same wear behaviour.

In this case as well (i.e. D = 15 μm), the optimum wear resistances were reflected by the AF–EP and AF–PK systems when the fibres were in the N orientation. For all the fibre/matrix systems a lower coefficient of friction was measured for the less abrasive case. In contrast, the neat matrices showed a higher coefficient of friction for the less abrasive case.

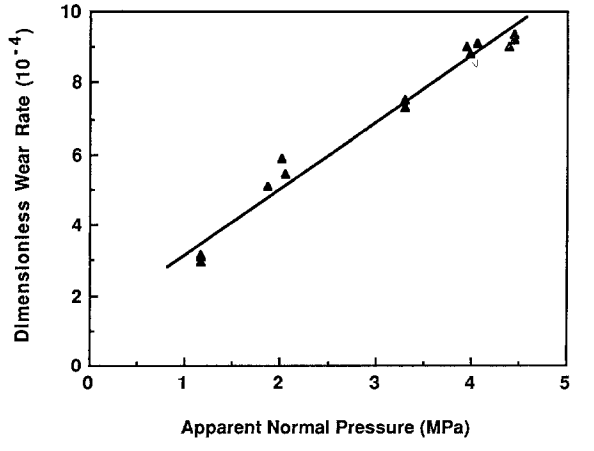

Figure 7 Dimensionless wear rate plotted against apparent normal pressure. CF–EP parallel orientation, V = 300 mm min^{-1}, A = 3 mm × 3 mm, D = 70 μm SiC.

TABLE II Dimensionless wear rates of the AF–EP and CF–PK systems sliding against D = 70 μm waterproof and non-waterproof type SiC abrasive paper

		Dimensionless wear rate, W (10^{-4})	
		Waterproof (D = 70 μm)	Non-waterproof (D = 70 μm)
AF–EP	N	1.04	0.75
	P	9.41	7.69
	AP	7.45	6.61
CF–PK	N	4.87	5.05
	P	4.63	5.52
	AP	7.60	8.59

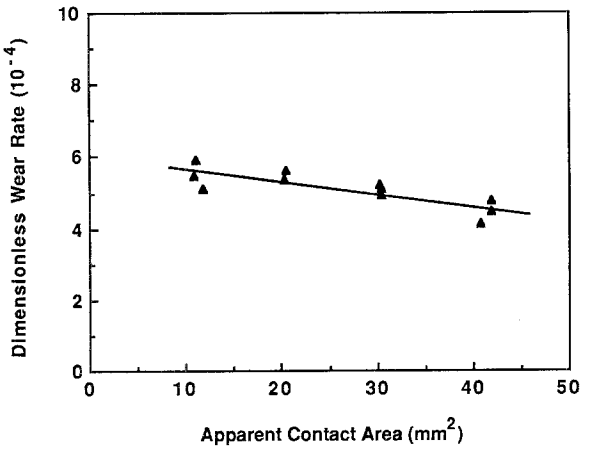

Figure 9 Dimensionless wear rate plotted against apparent contact area. CF–EP parallel orientation, $p = 2.2$ MPa, $V = 300$ mm min^{-1}, $D = 70\,\mu$m SiC.

4. Microscopic analysis of wear mechanisms

4.1. Unreinforced polymer matrices

The worn surface of PK was characteristic of relatively ductile materials. As shown in Fig. 13a, its surface was plastically deformed interspersed with plowed furrows parallel to the sliding direction. Wear debris was formed by the subsequent microcutting mechanism which is necessary to separate the plowed material from the surface. The PK was absent of the microcracking mechanism unlike the more brittle EP where undeformed pieces were immediately formed and removed from the surface. Fig. 13b shows the microcracking mechanism occurring on the worn surface of EP. Microcracks on the surface and small undeformed chips of the epoxy can be seen.

4.2. Glass and carbon fibre composites

Under low magnification, a general overview of the worn surfaces of the composite material systems can be developed. It was observed that different forms of wear mechanisms dominated for each of the main orientations (N, P and AP). With respect to each of the orientations, the worn surfaces of the CF–EP and GF–EP systems look similar with a few minor but important differences (Fig. 14). In principle, worn surfaces of the CF–PK system looked similar to those of the CF–EP and GF–EP systems except for the existence of plastically deformed matrix material between the damaged fibres as can be seen in Fig. 15.

Characteristic details of the abraded surfaces and subsurface regions found under higher magnification are illustrated in Fig. 16. For the N orientation case, it was observed that the fibre ends were cut or fractured by the abrasive particles in a slicing manner (Fig. 16a). For the CF–EP and CF–PK systems, the average length of the cut fibre pieces was greater than the original carbon fibre diameter, whereas for the GF–EP system, the cut fibre pieces had an average length less than the original glass fibre diameter. The profiles of the abraded materials contained a subsurface damage zone. In this zone, fibre/matrix debonding occurred along with the bending of fibres in the direction of sliding which caused fibre fracture and cracking (Fig. 16d). The subsurface damage zones of the CF–EP and CF–PK were deeper than that of the GF–EP. In the P orientation, fibre fracture occurred in the contact region as well as in the subsurface region (Figs 16b and e). Fibre removal from the contact region was enhanced by the plowing and cutting of the matrix between the exposed fibres. Delamination cracking took place in the subsurface up to a depth of about two to three fibre layers. In the AP orientation, fibre or fibre bundles were broken from the surface due to a bending action imposed by passing abrasive particles (Fig. 16c). The fibres were then subsequently removed separately or as whole fibre bundles after fibre/matrix separation occurred (Fig. 16f). The subsurface damage zone consisted mainly of fibre/matrix delaminations occurring up to a depth of two to three fibre layers. The dominant wear mechanisms which occurred in the composite materials under severe abrasion are schematically illustrated in Fig. 17.

4.3. Aramid fibre reinforced epoxy

The AF–EP system had a distinctively different wear surface appearance when compared to that of the CF–EP, GF–EP and CF–PK systems (Fig. 18). The aramid fibres in the N orientation acted as crack inhibitors. That is, the worn surface did not exhibit the microcracking mechanism which was present in all of the other expoxy systems (Fig. 18a). The abraded surface is similar to that of a ductile material being dominated by the microplowing mechanism. Fibre rupture beneath the surface could not be distin-

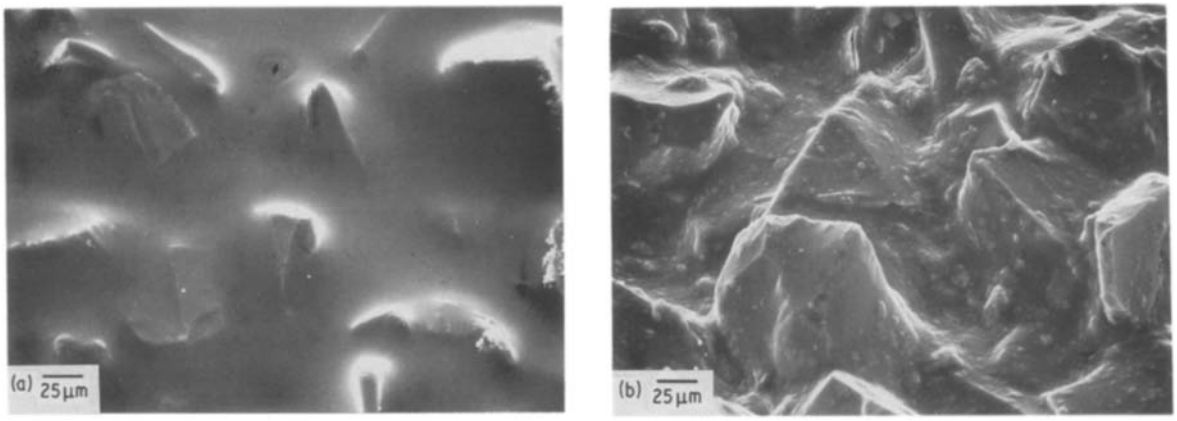

Figure 10 Scanning electron micrographs of (a) waterproof and (b) non-waterproof type SiC abrasive paper ($D = 70\,\mu$m).

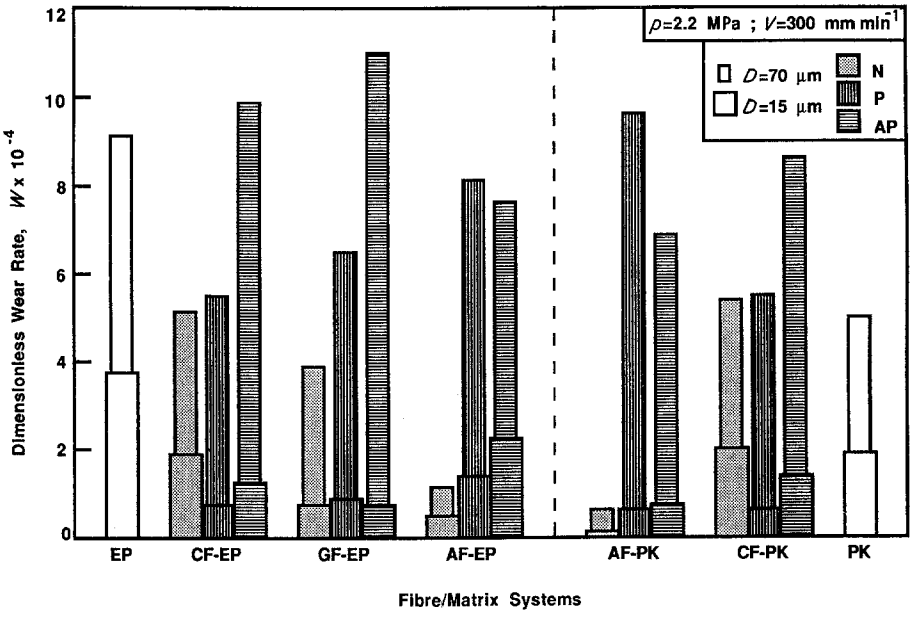

Figure 11 Averaged dimensionless wear rates of the fibre/matrix systems for the $D = 70$ and $15\,\mu m$ cases. (Not measured for the AF–PK system.)

guished. In the P orientation, the worn AF–EP did not exhibit brittle fibre fracture. Instead, fibres were completely peeled away from the surface and subsequently fibrillated (Fig. 18b). The subsurface damage zone was very shallow as can be seen in Fig. 18e. The AP orientation showed a high degree of fibrillation of the fibres at the site where they were torn apart by passing abrasive particles (Fig. 18c). Separation of the fibres from the surface occurred along the fibre/matrix interface. Again, the subsurface damage zone was shallow, about one fibre layer deep (Fig. 18f). The micro-wear mechanisms in the AF–PK system are, in principle, similar to those found in the AF–EP system and are, therefore, not described in further detail.

4.4. Effect of smaller particle size

Similar types of micro-wear mechanisms were observed for the $D = 15\,\mu m$ case; however, the mechanisms discussed earlier were not as pronounced. This resulted in lower material removal from the surface of the composites generating lower wear rates. The two neat matrices showed a lower amount of damage where the plowed furrows of the PK were more shallow and the fractured fragments from the EP surface were of a smaller dimension.

In the case of the CF–EP, GF–EP and CF–PK systems a lower amount of fibre fracture occurred, and the fibres were usually removed from the surface as partial pieces as opposed to entire sections of the fibre being removed (Fig. 19). In principle, the worn surfaces of these composites consisted of similar types of micro-wear mechanisms in each orientation. A slight difference occurred in the abraded surfaces of the CF–PK where plastically deformed matrix material existed between the damaged fibres. Again, the AF–EP system showed a different wear surface to that of the other three systems as it did in the case with the more abrasive paper. However, the peeling and fibrillation of the fibres were less pronounced (Fig. 20).

5. Discussion

The microcracking mechanism induces a higher degree of material removal as compared to the microplowing and microcutting mechanisms. This is verified by comparing the wear behaviour of PK and EP. The PK possessed a lower wear rate and the microcracking mechanism was absent. Regarding the composite systems, the anisotropic wear behaviour can be explained by observing the interactions between SiC particles and fibres. In the N orientation, the major contribu-

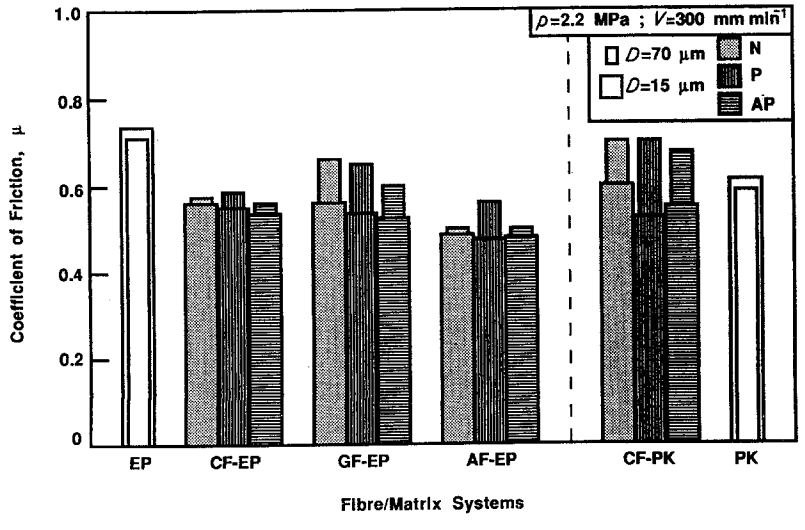

Figure 12 Averaged coefficients of friction of the fibre/matrix systems for the $D = 70$ and $15\,\mu m$ cases.

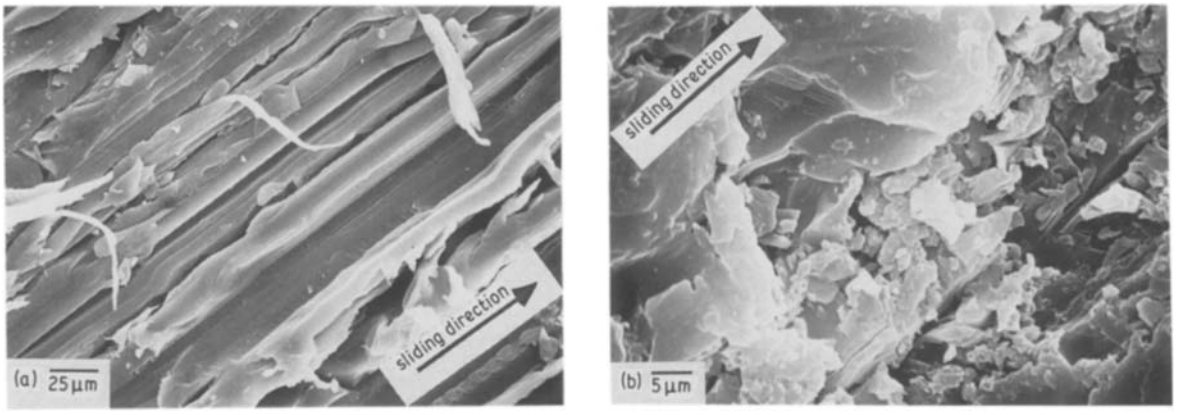

Figure 13 Scanning electron micrographs of (a) PK and (b) EP surfaces slid against $D = 70\,\mu m$ waterproof-type SiC paper.

tion for material removal was caused by the abrasive particle cutting the fibre ends in a slicing manner. A secondary contribution resulted from a pull-out action imposed on the fibres by passing abrasive particles. This contribution is enhanced by fibre fracture in the subsurface region due to a bending action which is simultaneously imposed by the passing particles. However, this process is inhibited by the presence of adjacent fibres. The GF–EP system had a lower wear rate than that of the carbon fibre systems in the N orientation. From the scanning electron micrographs it was observed that the cut glass fibre pieces were of a smaller dimension than the cut carbon fibre pieces and the subsurface damage zone was not as deep as in the carbon fibre systems. Glass fibres are isotropic and have an amorphous microstructure, whereas the microstructure of the carbon fibres consists of carbon atoms covalently bonded in layers parallel to the fibre axis but with relatively weak bonding between the layers in the radial direction [18]. This gives way to weak planes for sites of cleavage running axially resulting in larger cut fibre pieces.

In the P and AP orientations, the fibres are susceptible to damage caused by fibre–particle interactions. In the P orientation, fibre damage is enhanced by the abrasive particles plowing and cutting the matrix material between the exposed fibres increasing fibre/matrix debonding. The AP orientation generally showed a higher wear rate due to the in-plane bending imposed on the fibres by passing abrasive particles. The frequency of fracture (i.e. the number of fracture events per sliding distance) is higher for this case. Therefore, the time to break up fibres into a length l_c (the characteristic length necessary to remove the fibre out of the surface) is shorter resulting in more material removal per sliding distance.

The absence of the microcracking mechanism in the AF–EP and AF–PK systems created different wear surface and subsurface appearances. Microscopy on the N orientation case indicated the absence of secondary effects like interfacial cracking and removal of whole fibre parts typical of other composite systems. This suggests that the wear behaviour in this case is mainly determined by the wear resistance of the fibre material itself. In the P orientation, the relatively ductile behaviour of the fibre and the poor fibre/matrix bond quality enabled passing abrasive particles

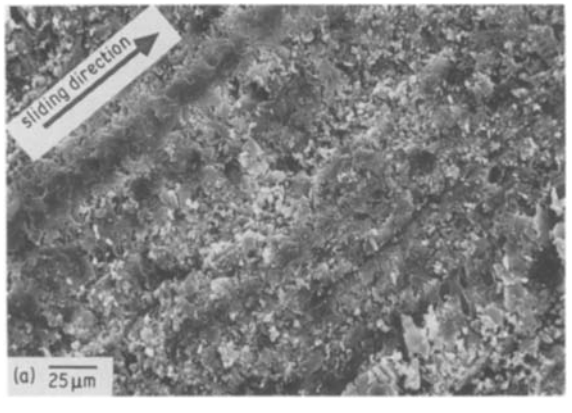

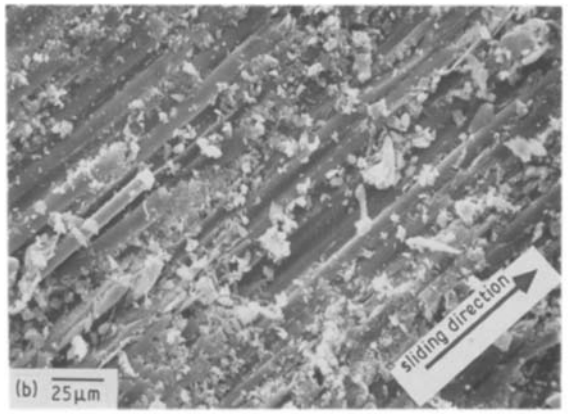

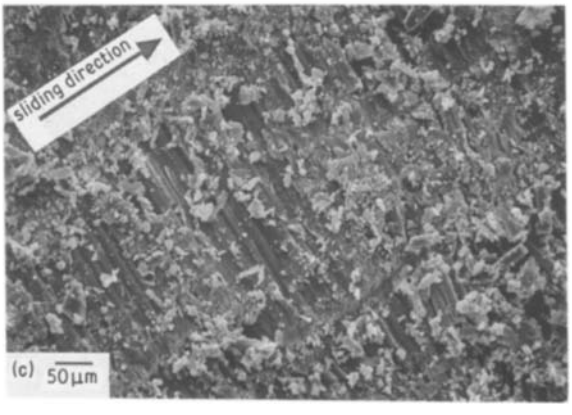

Figure 14 Low magnification scanning electron micrographs of GF–EP surfaces slid against $D = 70\,\mu m$ waterproof-type SiC paper: (a) N orientation, (b) P orientation, and (c) AP orientation.

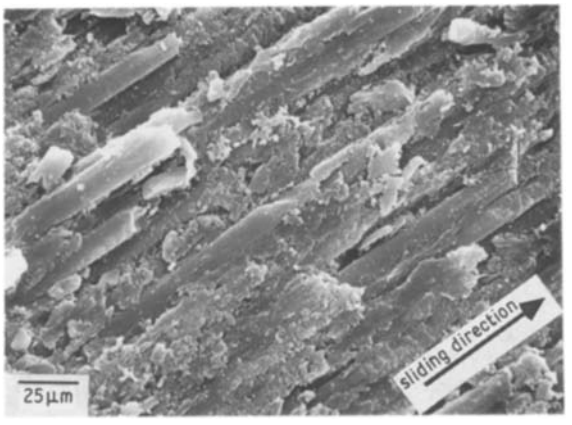

Figure 15 Low magnification scanning electron micrograph of CF–PK surface slid against $D = 70\,\mu m$ waterproof-type SiC paper in the P orientation.

to easily debond fibres from the surrounding matrix. The passing abrasive particles bent the fibres by almost 180 deg and peeled them out of their matrix beds as long as fibre–particle contact existed. This resulted in long fibre pieces as seen in the scanning electron micrographs. The following particles easily picked up the torn out fibres and continued to peel them out of the matrix until the complete fibre was removed from the surface. Therefore, the time to remove a fibre from the surface is much shorter in the AF–EP system than in the cases where fibres must be broken into many pieces before final removal can take place (CF–EP, GF–EP and CF–PK systems). Hence, a higher wear rate was measured for the aramid fibre reinforced systems in the P orientation relative to the other systems. A slightly different situation existed for the AP orientation case. The fibres were plastically

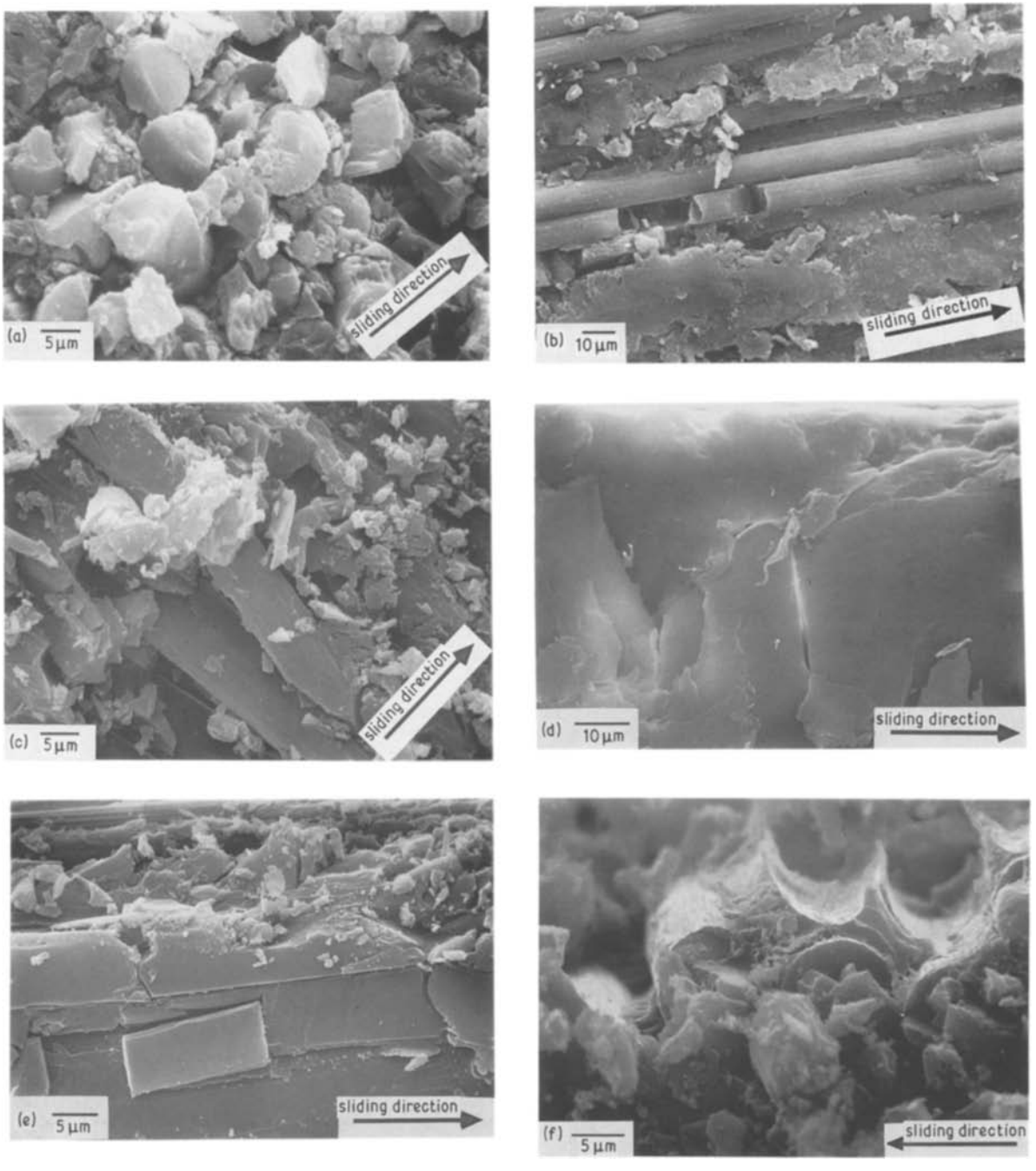

Figure 16 Scanning electron micrographs of the CF–EP system slid against $D = 70\,\mu m$ waterproof-type SiC paper. Surfaces (a) N orientation, (b) P orientation and (c) AP orientation; and subsurfaces (d) N orientation, (e) P orientation and (f) AP orientation.

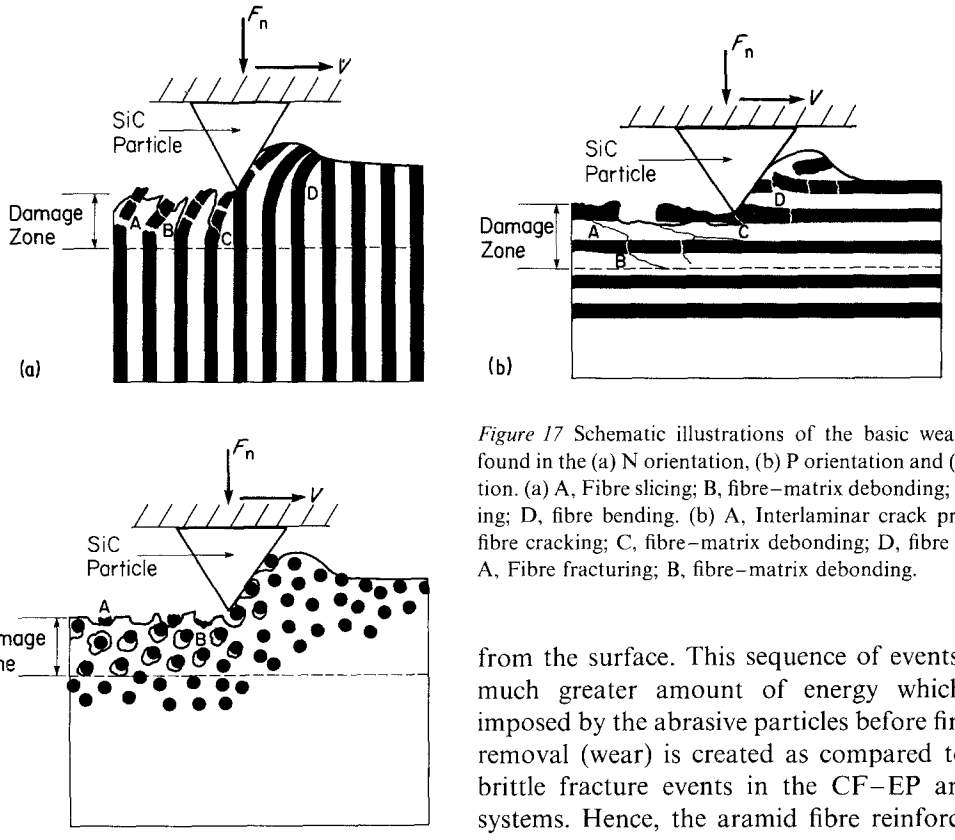

Figure 17 Schematic illustrations of the basic wear mechanisms found in the (a) N orientation, (b) P orientation and (c) AP orientation. (a) A, Fibre slicing; B, fibre–matrix debonding; C, fibre cracking; D, fibre bending. (b) A, Interlaminar crack propagation; B, fibre cracking; C, fibre–matrix debonding; D, fibre fracturing. (c) A, Fibre fracturing; B, fibre–matrix debonding.

deformed to a high degree by the in-plane bending load imposed on them by the passing abrasive particles. Finally, the fibres ruptured but remained attached to the surface. Subsequent fibrillation of the adhering fibres occurred before they were removed from the surface. This sequence of events requires a much greater amount of energy which must be imposed by the abrasive particles before final material removal (wear) is created as compared to the more brittle fracture events in the CF–EP and GF–EP systems. Hence, the aramid fibre reinforced systems exhibited a relatively lower wear rate in the AP orientation.

The wear behaviour of the composite materials was characterized by measuring wear rates under a specified tribological system. A network of wear data was created for the materials with respect to three material

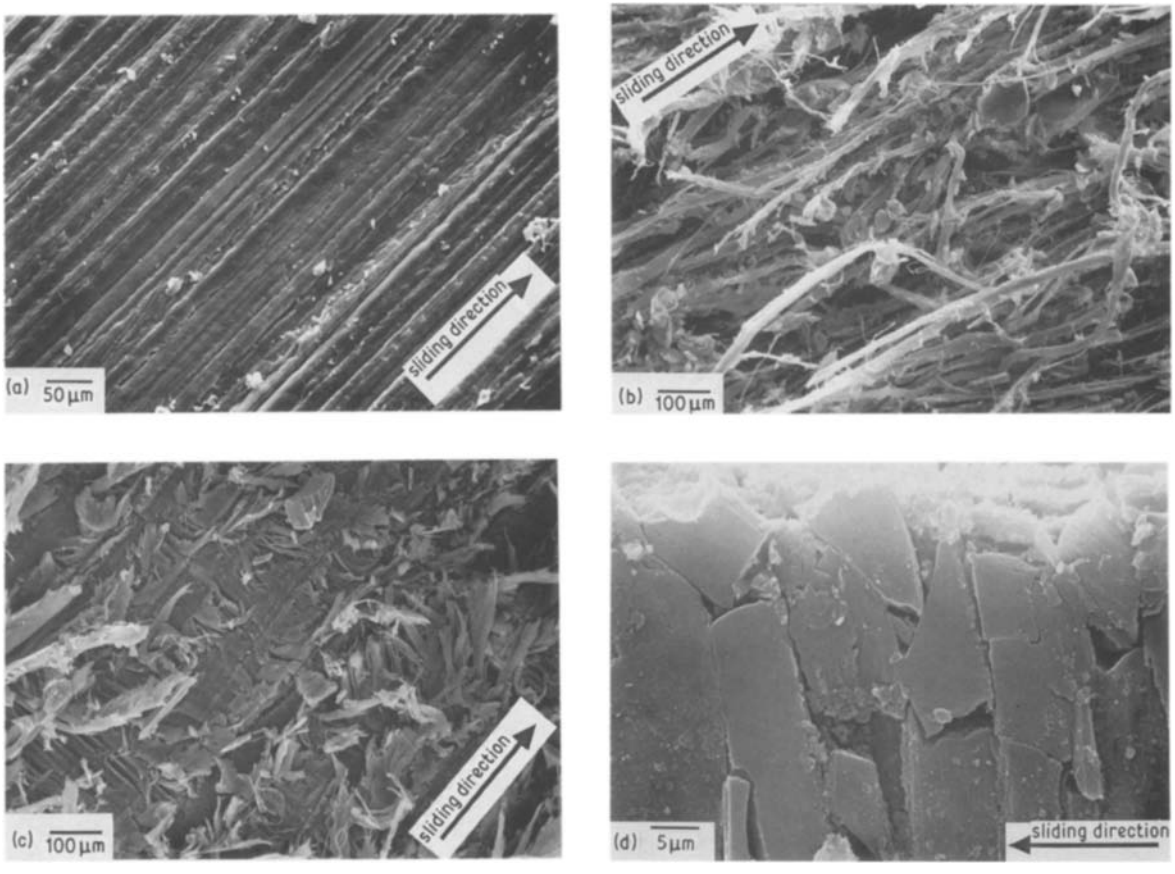

Figure 18 Scanning electron micrographs of the AF–EP system slid against $D = 70\,\mu m$ waterproof-type SiC paper. Surfaces (a) N orientation, (b) P orientation and (c) AP orientation; and subsurfaces (d) N orientation, (e) P orientation and (f) AP orientation.

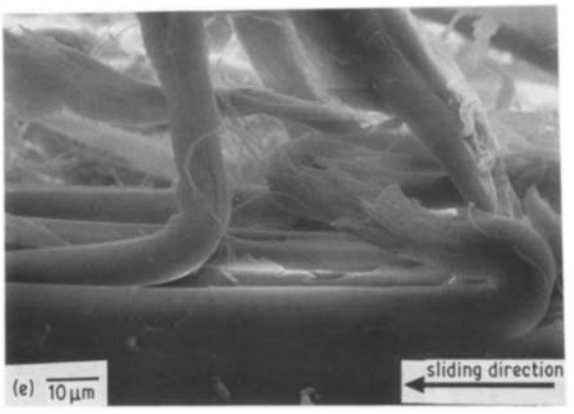

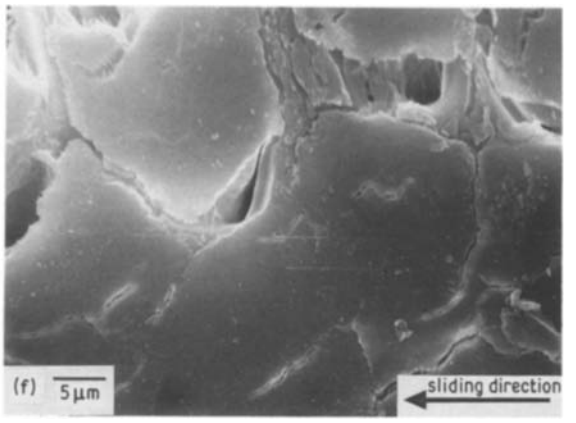

Figure 18 continued.

parameters: fibre orientation, fibre material and matrix material. Ideally, a systematic selection of the optimum variation of each parameter can be accomplished in order to develop a low wear composite material. Table III tabulates the wear resistance of the composite systems relative to that of the EP as a function of the material parameters. A potential low wear model material would consist of a PEEK matrix incorporating aramid fibres oriented normal to the contacting surface and carbon fibres oriented parallel to the contacting surface. This is schematically illustrated in Fig. 21.

6. Conclusions

The investigation of the wear behaviour of continuous fibre polymer composites resulted in three main sources of information. First, the effects of the operation variables applied load, sliding velocity and apparent contact area on the friction and wear characteristics of the composite materials were observed. As apparent normal pressure increased the coefficient of friction was not significantly changed while the dimensionless wear rate increased in a linear fashion. A variation in the sliding velocity did not have a significant effect on either the coefficient of friction or the dimensionless wear rate. Increasing the apparent contact area did not significantly effect the coefficient of friction, but the dimensionless wear rate slightly decreased. Second, through microscopic observations of the worn surfaces and subsurface regions, basic wear mechanisms were identified in each orientation. The varying ability of each mechanism to remove material resulted in the anisotropic wear behaviour. Observation of the fibre–abrasive particle interactions allowed for the differentiation of the dominating wear mechanisms. Fibre ends were cut in a slicing manner by passing abrasive particles when the fibres were oriented normal to the sliding surface. Plowing and cutting of the matrix material between fibres which were oriented parallel to the sliding direction enhanced fibre removal. In-plane bending of fibres caused fibre fracture and cracking resulting in a relatively higher wear removal when the fibres were oriented perpendicular to the sliding direction and parallel to the sliding surface. The amount of material removal of these mechanisms also varied for the different fibre and matrix materials producing different wear rates among

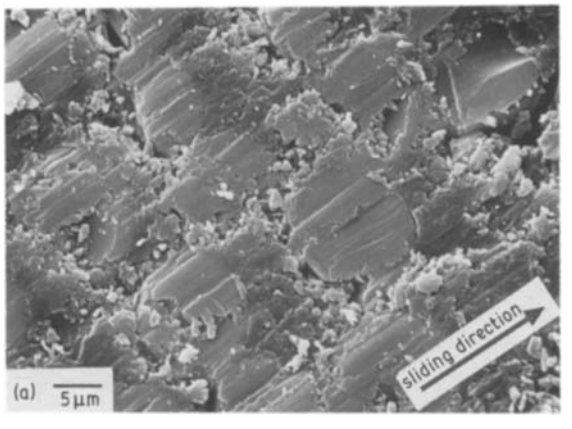

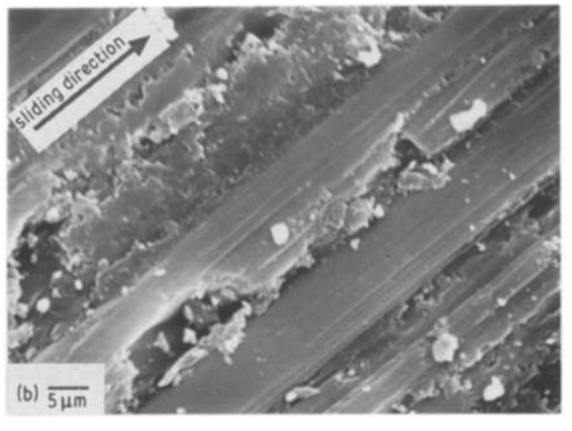

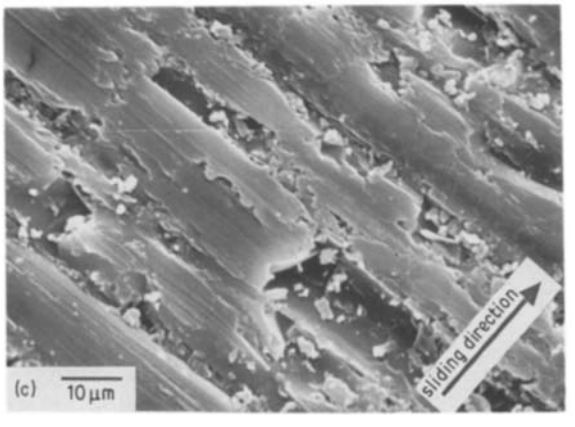

Figure 19 Scanning electron micrographs of the GF–EP surfaces slid against $D = 15\,\mu m$ waterproof-type SiC paper (a) N orientation, (b) P orientation and (c) AP orientation.

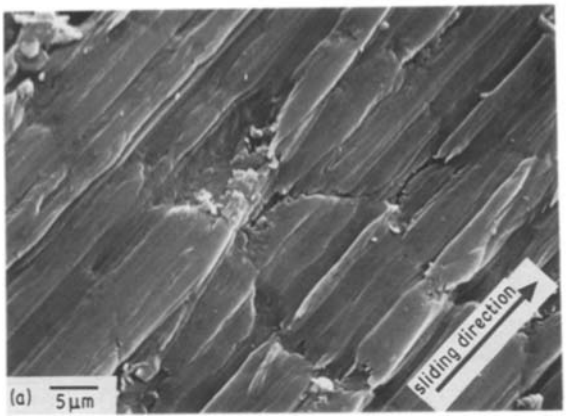

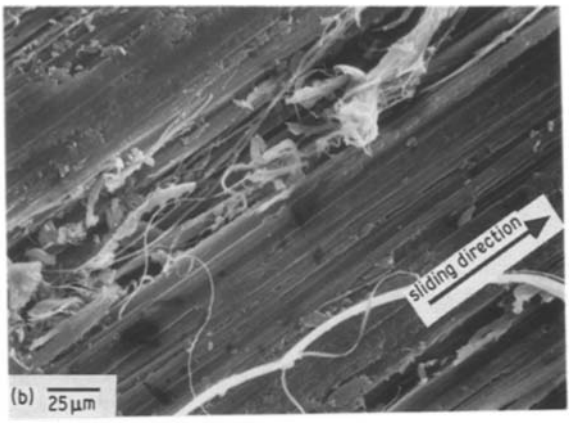

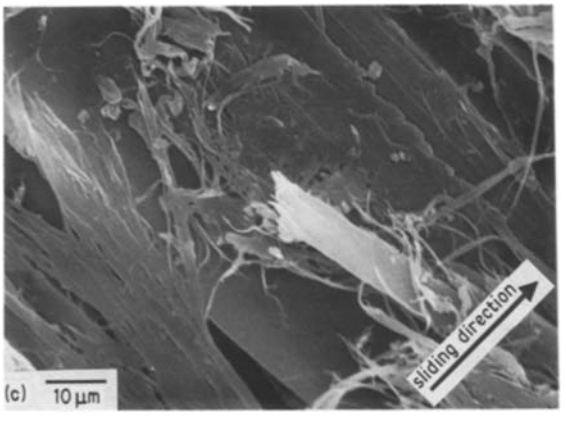

Figure 20 Scanning electron micrographs of the AF–EP surfaces slid against $D = 15\,\mu m$ waterproof-type SiC paper (a) N orientation, (b) P orientation and (c) AP orientation.

the composite systems. The third source of information was the compilation of a network of data on the wear behaviour of the composite materials with respect to three material parameters: fibre orientation, fibre material and matrix material. This led the way towards the systematic selection of an ideal low wear composite material which would consist of a PEEK matrix reinforced with aramid fibres oriented normal to the contacting surface and carbon fibres oriented parallel to the contacting surface.

These three sources of information were ascertained from the fundamental approach which was taken towards the selected composite materials in order to characterize their friction and wear behaviour. This information should serve as a data base which will aid in the understanding and evaluation of more complex composite materials operating in various tribological systems.

Acknowledgements

The authors would like to thank the staff at the Center for Composite Materials for the use of their facilities for the friction and wear tests. Thanks are also given to the staff of the Polymer and Composites Group at the Technical University of Hamburg-Harburg in West Germany for the use of their facilities especially for the extensive SEM work. Part of the work on the PEEK materials at Hamburg was supported by the Deutsche Forschungsgemeinschaft (DFG-FRI-675-1-1).

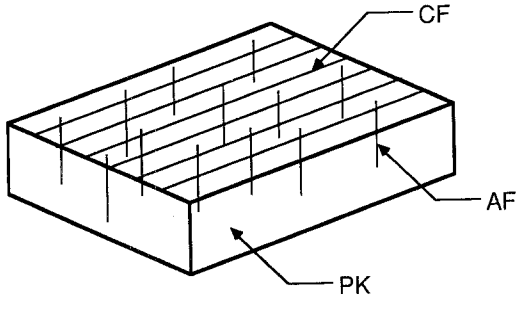

Figure 21 Illustration of the ideal low wear composite.

References

1. J. C. ANDERSON, *Tribology Int.* **10** (1982) 255.
2. H. M. HAWTHORNE, in Wear of Materials-1983, edited by K. C. Ludema (American Society of Mechanical Engineers, New York, 1983) p. 576.
3. V. K. JAIN, *Wear* **92** (1983) 279.
4. J. K. LANCASTER, *Tribology Int.* **12** (1973) 219.
5. R. RAMESH, KISHORE and R. M. V. G. K. RAO, *Wear* **89** (1983) 131.
6. N-H SUNG and N. P. SUH, *ibid.* **53** (1979) 129.
7. T. TSUKIZOE and N. OHMAE, *Fibre Sci. Tech.* **18** (1983) 265.
8. K. TANAKA, *J. Lub. Tech.* **99** (1977) 409.
9. J. K. LANCASTER, *Wear* **14** (1969) 223.
10. J. C. ROBERTS and H-W. CHANG, *ibid.* **79** (1982) 363.
11. H. SIN, N. SAKA and N. P. SUH, *ibid.* **55** (1979) 163.
12. J. M. THORP, *Tribology Int.* **4** (1982) 59.
13. K. FRIEDRICH and J. C. MALZAHN, in Wear of Materials-1983, edited by K. C. Ludema (American Society of Mechanical Engineers, New York, 1983) p. 604.
14. C. LHYMN, K. E. TEMPELMEYER and P. K. DAVIS, *Composites* **2** (1985) 127.
15. K. FRIEDRICH (ed.), "Friction and Wear of Polymer Composites" (Elsevier, Amsterdam, 1986).

TABLE III Wear resistance ratios of the composite materials with respect to material parameters

Matrix		Reinforcing fibre			
		CF	GF	AF	Neat
EP	N	1.8	2.3	7.9	1
	P	1.7	1.4	1.1	
	AP	0.9	0.8	1.2	
PK	N	1.7	–	15.2	1.8
	P	1.6	–	0.9	
	AP	1.0	–	1.3	

Wear resistance ratio $= \frac{W_c^{-1}}{W_{ep}^{-1}}$

16. R. TURNER and F. N. COGSWELL, in Proceedings of the 18th International SAMPE Technical Conference, 1986, p. 32.
17. M. CIRINO, Masters Thesis, University of Delaware, Mechanical and Aerospace Engineering, December 1985.
18. N. J. PRARATT, "Fibre-Reinforced Materials Technology" (Von Nostrand Reinhold, London, 1972) p. 69.

Received 15 August
and accepted 23 September 1986